Structure and stability of ZrSiO4 under hydrostatic pressure

Marques, M.; Florez, M.; Recio, J.M.; Gerward, Leif; Olsen, J. Staun

Published in:
Physical Review B Condensed Matter

Link to article, DOI:
10.1103/PhysRevB.74.014104

Publication date:
2006

Document Version
Publisher's PDF, also known as Version of record

Structure and stability of $ZrSiO_4$ under hydrostatic pressure

M. Marqués, M. Flórez, and J. M. Recio*
Departamento de Química Física y Analítica, Universidad de Oviedo, E-33006 Oviedo, Spain

L. Gerward
Department of Physics, Technical University of Denmark, 2800 Kongens Lyngby, Denmark

J. Staun Olsen
Niels Bohr Institute, Oersted Laboratory, 2100 Copenhagen, Denmark

(Received 7 November 2005; revised manuscript received 5 April 2006; published 14 July 2006)

We present the results of a combined experimental and theoretical investigation aimed to determine structural and equation-of-state parameters and phase stability thermodynamic boundaries of $ZrSiO_4$ polymorphs. Experimental unit-cell data have been obtained for a powdered sample in a diamond-anvil cell using energy-dispersive synchrotron x-ray diffraction with emphasis on the pressure range 0–15 GPa. Static total-energy calculations have been performed within the density functional theory at local density and generalized gradient approximation levels using a plane-wave pseudopotential scheme. Our quantum-mechanical simulations explore the pressure response of the two observed tetragonal structures (zircon- and scheelite-type reidite) as well as of other potential post-scheelite polymorphs up to about 60 GPa. We find very good agreement between our experimental and calculated pressure-volume values for the low-pressure phase of $ZrSiO_4$. A microscopic analysis of the bulk compressibility of zircon and reidite in terms of polyhedral and atomic contributions is proposed to clarify some of the discrepancies found in recent theoretical and experimental studies. Our results show the relevant role played by the oxygen atoms in the description of this property. The zircon-reidite equilibrium phase transition pressure is computed around 5 GPa. No other post-scheelite phase is found stable above this pressure though a decomposition into ZrO_2 (cottunite) and SiO_2 (stishovite) is predicted at about 6 GPa. These two transition pressure values are well below the experimental ranges detected in the laboratory in concordance with the large hysteresis associated with these transformations.

DOI: 10.1103/PhysRevB.74.014104 PACS number(s): 64.30.+t, 64.70.−p, 61.10.−i, 71.15.Nc

I. INTRODUCTION

Understanding the behavior of materials exposed to variable thermodynamic conditions and chemical agents rests in many instances on detailed knowledge of the correlation between their observable properties and the local geometry and interactions around their constitutive atoms. The particular structural and chemical features of the bonding network in $ZrSiO_4$ provide a paradigmatic case to investigate this correlation. This mixed oxide presents simultaneously two nominally 4+ cations, shows the lowest compressibility for a material containing SiO_4 tetrahedra, contains interstices appropriate for hosting and retain rare-earth elements, and exhibits an anomalous and possibly unique displacive mechanism regarding silicate solid-solid transformations.[1]

A straightforward strategy to study the physics and chemistry of the local environment of atoms in crystalline solids is the application of hydrostatic pressure. The equations of state (EOS) of the two observed tetragonal polymorphs of $ZrSiO_4$, zircon and reidite, have been the subject of recent experimental and theoretical investigations. Contrarily to previous data of the zero-pressure bulk modulus for zircon ($B_0 \simeq 230$ GPa),[2] van Westrenen *et al.*[3] and Ono *et al.*[4] obtained values around 10% lower. In addition, Ono *et al.*[4] pointed out that the main reason for the difference between their B_0 value for reidite (392±9 GPa) and that reported by Scott *et al.* (301.4±12.5 GPa) is the nonhydrostaticity of the medium in the high-pressure experiments of these authors.[5] Scott *et al.* claimed that their results in the hydrostatic regime are completely indistinguishable from the higher-pressure results.

The compressibility of both structures has been also analyzed in terms of their elementary polyhedra which in both lattices are nonregular SiO_4 tetrahedra and ZrO_8 triangular dodecahedra (see Refs. 6 and 7, and references therein). For the zircon phase, Hazen and Finger concluded that its remarkable incompressibility is mainly due to the ZrO_8 polyhedra with $B_{ZrO_8,0} \simeq 280$ GPa, whereas $B_{SiO_4,0}$ has a surprisingly low value around 225 GPa.[2] Smyth *et al.* recommended in this respect that "the anomalous results of Hazen and Finger" should be reexamined.[8] The lack of polyhedral compressibilities in the reidite structure makes it also worth performing a polyhedral analysis in this structure. Contrarily to zircon, the high B_0 value of reidite is achieved by the low compressibility of SiO_4 tetrahedra according to the experiments of Scott *et al.*[5]

Zircon and reidite show strong structural anisotropy under temperature and pressure as manifested by the different values of their corresponding linear expansion coefficients and linear compressibilities.[6] With respect to pressure effects, the observed behavior can be summarized as follows: (i) reidite is less anisotropic than zircon, and (ii) the compressibility along the *a* axis is greater than that along the *c* axis in zircon whereas the opposite result is found in reidite. The structural anisotropy can be traced back as due to the orientation and linkage of the constitutive polyhedra and, ultimately, to the disposition of Si-O, Zr-O, and O-O bonds. In the explanation

given by Smyth *et al.*[8] (later quoted in the review of Finch and Hanchar[6]), we have found that Zr-O bond strengths are not correctly correlated with the observed linear compressibilities.

The last issue that has attracted our interest in this contribution is the determination of pressure and temperature ranges of stability for zircon and reidite. Static-pressure[1,3,4,9,10] and shock-wave compression[11–13] experiments have identified reidite as the only high-pressure polymorph of $ZrSiO_4$. At elevated temperature and pressure, $ZrSiO_4$ is observed to decompose into SiO_2 (stishovite) and ZrO_2 (cottunite).[14] Due to the high energetic barriers associated with the hysteresis of these processes, the equilibrium thermodynamic boundaries are not well constrained though positive Clapeyron p-T slopes for both transitions are suggested.[6,14]

In this study, we aim to contribute to the understanding of the structural and stability behavior of $ZrSiO_4$ under hydrostatic pressure. Diamond-anvil cell experiments using energy-dispersive synchrotron x-ray diffraction in powdered samples and static total-energy calculations based on the density functional approximation were carried out in the pressure ranges 0–15 GPa and 0–60 GPa, respectively. This combined experimental and theoretical investigation allows us to clarify some of the discrepancies found in previous works. In particular, we report and analyze in detail the EOS of zircon and reidite in terms of bond, polyhedral, and linear compressibilities with a special emphasis on a comparison with previous experimental data. Furthermore, we obtain atomic compressibilities from the topology of the crystalline electron densities. The second objective of our study is to characterize the thermodynamics of the zircon→reidite and reidite→SiO_2 (stishovite)+ZrO_2 (cottunite) transformations. Equilibrium transition properties are evaluated and the effects of the temperature on the thermodynamic boundaries are analyzed. Finally, two potential post-scheelite polymorphs (fergursonite- and wolframite-type structures) are also discussed.

The present paper is organized in three more sections. Next, a brief description of the experimental and computational procedures is given. Section III A contains the structural and EOS results of zircon and reidite, and Secs. III B and III C the polyhedral and atomic [in terms of Bader's atoms in molecules (AIM) formalism[15]] analyses of these properties. Phase transition properties and stability ranges of $ZrSiO_4$ polymorphs are presented in Sec. III D. The paper ends with the main conclusions of our work.

II. EXPERIMENTAL METHODS AND COMPUTATIONAL DETAILS

A. Experimental methods

The zircon sample used in the present work has been purchased from Strem Chemicals Inc. According to the manufacturer, the product is typically 99+% pure. The major impurities are iron oxide, aluminum oxide, and zirconium oxide. The sample comes in the form of a white powder.

High-pressure powder x-ray diffraction patterns were recorded at room temperature using the white-beam method and synchrotron radiation at Station F3 of HASYLAB-DESY in Hamburg, Germany. The diffractometer, working in the energy-dispersive mode, has been described elsewhere.[16] High pressures were obtained in a Syassen-Holzapfel type diamond-anvil cell. A finely ground powder sample and a ruby chip were placed in a 200-μm-diam hole in an inconel gasket, pre-indented to a thickness of 60 μm. A 16:3:1 methanol:ethanol:water mixture was used as the pressure-transmitting medium. The pressure in the cell was determined from the wavelength shift of the ruby R_1 luminescence line and applying the nonlinear pressure scale of Mao *et al.*[17] The Bragg angle of each run was calculated from a zero-pressure spectrum of sodium chloride in the diamond-anvil cell.

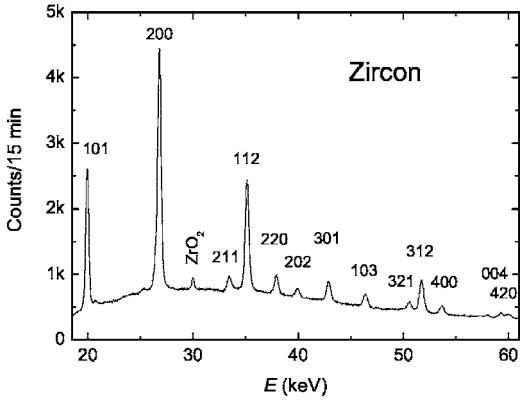

FIG. 1. Energy-dispersive x-ray diffraction spectrum of zircon at ambient pressure. The small peak at about 30 keV is due to zirconium oxide. The Bragg angle is θ=4.01°. The strong zirconium fluorescence lines (at 15.7 and 16.7 keV) are not shown.

Figure 1 shows an energy-dispersive x-ray diffraction spectrum of zircon. In a typical run, a series of spectra were recorded for a pressure increment of 1–2 GPa at a time. At each pressure, values for the lattice parameters and the unit-cell volume were derived and refined by a least-squares method, using the observed peak positions in the diffraction spectrum. The pressure-volume data were then described by the Birch-Murnaghan equation of state[18]:

$$p = \frac{3}{2}B_0(x^{-7/3} - x^{-5/3})\left(1 - \frac{3}{4}(4 - B_0')(x^{-2/3} - 1)\right), \quad (1)$$

where $x = V/V_0$, V is the volume per formula unit at pressure p and V_0 is the corresponding volume at zero pressure. The least-squares fitting parameters are the bulk modulus and its pressure derivative evaluated at zero pressure (B_0 and B_0', respectively).

B. Computational details

Total-energy calculations at selected unit-cell volumes of zircon, reidite, fergusonite-type, wolframite-type, stishovite (SiO_2), and cottunite (ZrO_2) structures were performed under the framework of the density functional theory using the Vienna *ab initio* simulation package (VASP) code[19] in connection with the projector-augmented wave (PAW) method.[20] The exchange and correlation energy was treated via the lo-

TABLE I. Summary of zero-pressure structural and cohesive properties of zircon and reidite. a and c in Å, V_0 (volume per formula unit) in Å^3, and B_0 in GPa.

	Zircon					Reidite			
	Expt.[a]	Expt.[b]	Expt.[c]	LDA[d]	GGA[e]	Expt.[f]	Expt.[g]	LDA[d]	GGA[e]
a	6.6042	6.6058	6.601	6.599	6.704	4.734		4.723	4.788
c	5.9796	5.9772	5.975	5.959	6.040	10.510		10.411	10.640
x						0.28		0.2585	0.2584
y	0.0660			0.0661	0.0667	0.11		0.0927	0.0929
z	0.1951			0.1944	0.1953	0.055		0.0462	0.0476
V_0	65.20	65.20	65.10	64.87	67.86	58.88	57.78	58.06	60.97
B_0	227	201	225±8	231	201		392±9	258	221
B_0'	6.5	3.9	6.5±1.6	4.8	5.1		4	4.5	5.0

[a]Experimental. $ZrSiO_4$ nonmetamict natural (Ref. 2).
[b]Experimental. $ZrSiO_4$ synthetic pure (Ref. 3).
[c]Experimental. $ZrSiO_4$ synthetic pure (99+%) (This work).
[d]Calculated. LDA (This work).
[e]Calculated. GGA (This work).
[f]Experimental. Shock wave (Ref. 12).
[g]Experimental. Static (Ref. 4). V_0 extrapolated using EOS fitting.

cal density approximation (LDA) and the generalized gradient approximation (GGA) using the Perdew-Wang[21] and the Ceperley-Alder[22] parametrizations, respectively. In both cases, high-precision calculations with a cut off energy of 500 eV for the plane-wave basis and converged with respect to the k-point integration were performed. In particular, the Brillouin zone integrations were carried out using the special k-point sampling of the Monkhorst-Pack type[23] with $4\times4\times4$ grids. The optimization of the geometry at each volume was performed via a conjugate-gradient minimization of the total energy, using the Hellmann-Feynman forces on the atoms and stresses on the unit cell. For the energy calculation of the optimized crystal structures, the tetrahedron method with Blöchl correction was applied. In special, the total energies were converged to below 0.1 meV/atom and the geometry relaxation was considered to be completed when the total force on the atoms was less than 1 meV/Å.

In a second step, we convert the calculated energy-volume (per formula unit) points (E,V) into static (zero-temperature and zero-point vibrational contributions neglected) and finite-temperature pressure-volume (p,V) isotherms using numerical and analytical procedures coded in the GIBBS program.[24] Thermal contributions are included by means of a nonempirical quasiharmonic Debye-like model that only needs the set of (E,V) points and the calculated static bulk modulus to evaluate thermodynamic properties at different temperatures. We have found a good agreement between the results of several thermodynamic properties obtained within this model and those obtained by Fleche[25] in zircon using a more sophisticated procedure that involves explicit evaluation of Γ-point vibrational frequencies. However, due to the approximate character of the Debye model, we mainly focus on the static results, the effect of temperature being only considered qualitatively in the discussion of the transformation equilibrium boundaries. The main outcome of our simulation strategy is the pressure dependence (from 0 up to 60 GPa) of all the unit-cell parameters, atomic coordinates, polyhedral volumes, and Gibbs energies of the $ZrSiO_4$, SiO_2, and ZrO_2 structures.

Finally, using the AIM formalism[15] and the CRITIC program,[26] a microscopic analysis of the electron density of zircon and reidite has been carried out with the aim of evaluating the atomic contributions to the bulk compressibility. To this end, at the VASP equilibrium geometries we have generated all-electron wave functions from CRYSTAL calculations[27] using the same exchange and correlation functionals as in the pseudopotential ones. We have checked that the residual strains associated with the nonoptimized electron densities in the CRYSTAL calculations do not introduce significant modifications in the final atomic decomposition of the crystal compressibility. The AIM formalism allows the chemical characterization of the topology of the electron density in terms of (i) critical points where the gradient of the electron density is zero and (ii) nonoverlapping electronic basins surrounded by surfaces with a nil flux of the electron density gradient. Integrations within these basins lead to atomic volumes (V_i).

III. RESULTS

A. Structural properties and equations of state (EOS)

Zircon and reidite belong, respectively, to the $I4_1/amd$ and $I4_1/a$ space groups. Their conventional unit cells are tetragonal and contain 4 Zr and Si atoms at special positions [Zr at $4a(0,\frac{3}{4},\frac{1}{8})$ and $4b(0,\frac{1}{4},\frac{5}{8})$ and Si at $4b(0,\frac{3}{4},\frac{5}{8})$ and $4a(0,\frac{1}{4},\frac{1}{8})$, respectively] and 16 O atoms at $16h(0,y^z,z^z)$ and $16f(x^r,y^r,z^r)$, respectively. Both structures have been described in detail previously (see, for example, Refs. 6 and 7, and references therein). Our experimental and calculated lattice parameters (a and c) and oxygen coordinates at zero pressure are collected in Table I along with other representa-

tive experimental data. We found a good agreement between previous and present results. Notice that the expected underestimation of the structural parameters at the LDA level is only within 1%, whereas the GGA overestimates up to 4% the volume of $ZrSiO_4$ polymorphs. At the LDA level, the agreement between the theoretical and experimental values is very good for zircon and a little worse for reidite, the discrepancies probably being related to the effect of the residual strain in the shock-induced reidite sample.[12] In this respect, we must note that our calculated oxygen positions are closer to those of other scheelite-type compounds than the values determined by Kusaba *et al.*[12]

According to the experimental data reported in Refs. 2, 28, and 29, the room-temperature (RT) value of B_0 in zircon lays within a range of 225–230 GPa. Similar or higher values have been obtained using several computational techniques.[25,30–33] The evaluation of B_0 from the elastic constants experimentally determined by Ozkan *et al.*[34] gives also a value of 225.2 GPa. We refer to the data from all these works as set I. In set II, we include recent investigations of the compressibility of zircon in diamond anvil cells using x-ray diffraction techniques. In these experiments, van Westrenen *et al.*[3] and Ono *et al.*[4] have reported, respectively, 199±1 GPa and 205±8 GPa for B_0 at RT when they set B_0' to 4. In addition, GGA calculations of Farnan *et al.*[31] yield a slightly lower value (196 GPa). It should be pointed out that the effect of fixed or variable B_0' parameters does not explain the existence of these two sets of B_0 values around 225 GPa and 200 GPa, respectively. The origin of such discrepancies was analyzed in detail by van Westrenen *et al.*[3] who listed a number of factors affecting the experimental determination of the EOS parameters. Nevertheless, a clear conclusion could not be drawn to explain the existing discrepancies and a combination of effects was proposed.[3]

Our pressure-volume and pressure-normalized volume diagrams plotted in Fig. 2 (V_0 is the corresponding zero-pressure volume per formula unit of zircon) illustrate quantitatively the observed differences in the response of the unit-cell volume of zircon to hydrostatic pressure. First, the p-V diagram [Fig. 2(a)] shows an overall good agreement between our LDA p-V data and the experiments (in particular, those by van Westrenen *et al.*[3] up to around 15 GPa), the GGA calculations providing volumes about 5% higher. Second, the p-V/V_0 diagram [Fig. 2(b)] classifies more clearly the curves according to their B_0 values. It is apparent the very good agreement between our experimental and calculated LDA $(p, V/V_0)$ values, both yielding B_0 around 230 GPa and therefore supporting the data of set I. In the low-pressure range covered by the experiments of Ono *et al.*, the deviations from our experimental results are almost negligible, indicating that the error bars of the corresponding B_0 values should be taken into consideration. Larger discrepancies appear at increasing pressures with respect to the experimental values of van Westrenen *et al.*,[3] as expected from the two different values of B_0. Honestly speaking, we might remark that our GGA p-V/V_0 results are in fair agreement with the measured points of van Westrenen *et al.* and yield a B_0 value close to the data of set II. This result could reveal that it is delicate to decide for zircon the relevant experimental B_0 from our DFT calculations. Nevertheless, in the next subsections we will mainly make use of our LDA calculations as they provide a reasonable overall description of the structure, the compressibility, and the phase transition properties of $ZrSiO_4$. Results at the LDA level of computation have been also reported in our previous work on group-IV nitrides[35] using the same VASP methodology.

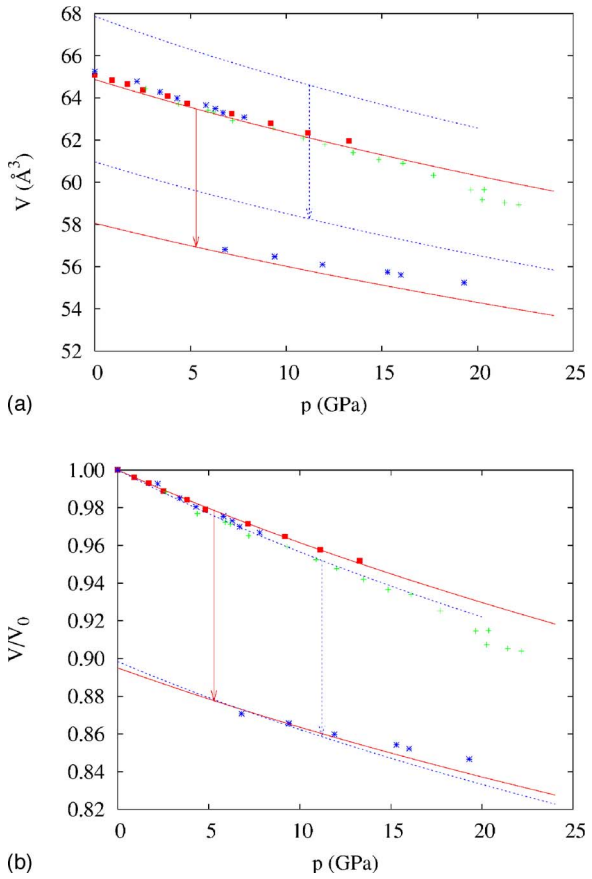

FIG. 2. (Color online) Volume (a) and normalized volume (b) versus pressure diagrams. Symbols stand for the experimental data of this work (solid squares), Ref. 3 (crosses), and Ref. 4 (stars). Standard deviations of the volume in the range 0.01–0.02 Å^3 (Ref. 3) and (most of the points) in the ranges 0.02–0.04 Å^3 (Ref. 4, zircon) and 0.03–0.08 Å^3 (Ref. 4, reidite). Lines correspond to our calculated data under the LDA (solid) and GGA (dashed) approximations. Arrows represent calculated volume collapses at the LDA and GGA zircon→reidite transition pressures (see Sec. III D).

For reidite, the difference between the two experimental values of B_0 [392±9 (Ref. 4) and 301.4±12.5 (Ref. 5)] is as large as around 100 GPa. These two values are much higher than our computed ones. GGA results produce definitively a too compressible scheelite-type polymorph, whereas our LDA value is around 14% lower than that reported by Scott *et al.* The particular $(p, V/V_0)$ data points of Ono *et al.* below 13 GPa do not show, however, large discrepancies with respect to our calculated values. Differences come from the rate V/V_0 decreases as pressure is applied. Notice that the zero-pressure volume of reidite by Ono *et al.* is not directly obtained in their experiments, but determined in the EOS fitting procedure. Their value is almost 2% lower than previous experimental data of Reid and Ringwood[9] and Kusaba *et al.*[12] which might be considered as a factor to overestimate

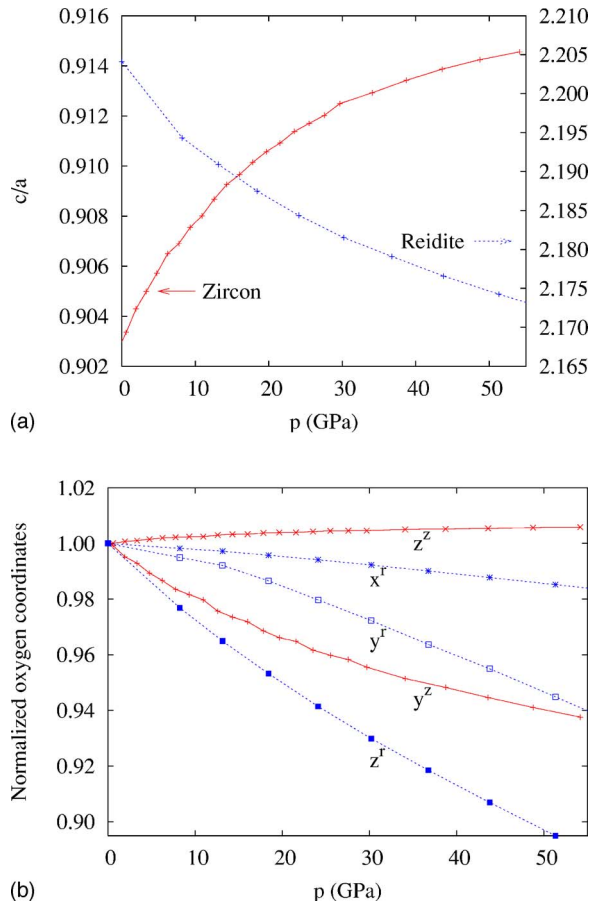

FIG. 3. (Color online) Pressure effects on (a) the c/a ratio and (b) the normalized oxygen coordinates for zircon and reidite polymorphs according to our LDA calculations.

B_0. In addition, estimations of the zero-pressure bulk modulus of ABO_4 compounds can be obtained by means of simple models relating B_0 with the volume V_0 and the formal charges of the A and B cations, Z_A and Z_B, respectively.[5,36,37] In this respect, we note that Errandonea *et al.*[36] found a linear relationship between B_0 and the $Z_A/\bar{d}^3_{A\text{-O}}$ quotient, $\bar{d}_{A\text{-O}}$ being the average A-O distance in the AO_8 polyhedron, of about 25% of the known ABO_4 scheelite and scheelite-related compounds. They used this relationship to predict a value of 220±40 GPa for B_0 of reidite which is in concordance with our LDA value (258 GPa). Nevertheless, it must be stressed that these types of simple relationships are strongly sensitive to the data set included in the fit and so the estimated bulk moduli should be treated with caution.

The structural anisotropy under pressure of the two $ZrSiO_4$ polymorphs can be measured in terms of observable properties as the linear compressibilities along the a and c axes, κ_a and κ_c, respectively. Opposite results are obtained for zircon and reidite. In agreement with the experimental data, a is more (less) compressible than c in zircon (reidite) and the degree of anisotropy of zircon under pressure is greater than that of reidite [see Fig. 3(a)]. Our calculated linear compressibilities for zircon at zero pressure ($\kappa_a = 1.68 \times 10^{-3}$ GPa^{-1} and $\kappa_c = 0.98 \times 10^{-3}$ GPa^{-1}) are similar to those determined by Hazen and Finger[2] ($\kappa_a = 1.6 \times 10^{-3}$ GPa^{-1} and $\kappa_c = 0.95 \times 10^{-3}$ GPa^{-1}). In reidite, our calculated values ($\kappa_a = 1.10 \times 10^{-3}$ GPa^{-1} and $\kappa_c = 1.69 \times 10^{-3}$ GPa^{-1}) show greater discrepancies with the values reported by Scott *et al.*[5] ($\kappa_a = 7.42 \times 10^{-4}$ GPa^{-1} and $\kappa_c = 1.08 \times 10^{-3}$ GPa^{-1}), though it is to be noted that the latter do not recover the value they reported for the bulk ($\kappa = 2\kappa_a + \kappa_c$). As pointed out by these authors, the low compressibility along the a axis in reidite has to be related to the repulsions between oxygen atoms whose shortest interatomic distances are found in the ab plane. Finally, pressure effects on the normalized oxygen positions in zircon and reidite polymorphs are shown in Fig. 3(b). With the exception of the z coordinate in zircon, we observe a decreasing of the O positions as pressure increases, the greatest relative diminutions being found for the z coordinate in reidite and the y coordinate in zircon. As we will see below, the pressure dependence of the oxygen coordinates is closely related to the way the polyhedra of the crystal are linked to each other and, consequently, controls the relation between the bulk and polyhedral compressibilities.

B. Polyhedral analysis of the structures

For our purposes, it is interesting to recall that distorted SiO_4 tetrahedra and distorted ZrO_8 triangular dodecahedra are present in both polymorphs. As pointed out by Mursic *et al.*,[38] "it is useful to describe the Zr-O polyhedral environment as two interpenetrating tetrahedra" that we denote as $ZrO_4(o)$ and $ZrO_4(p)$, the o and p labels indicating their oblate and prolate conformations. The degree of distortion of the SiO_4, $ZrO_4(o)$, and $ZrO_4(p)$ tetrahedra can be quantified by means of the quadratic elongation (λ) and angular variance (σ^2_θ) parameters proposed by Robinson *et al.*:[39]

$$\lambda_i = \frac{1}{4}\sum_{k=1}^{4}\left(\frac{d_{ki}}{d_{0i}}\right)^2, \quad \sigma^2_{\theta,i} = \frac{1}{5}\sum_{k=1}^{6}(\theta_{ki} - 109.47^\circ)^2, \qquad (2)$$

where d_{ki} and θ_{ki} stand for the bond lengths and angles of tetrahedron i, and d_{0i} is the center-to-vertex distance for a regular tetrahedron whose volume is equal to that of the distorted one.

A detailed structural characterization of all the cationic polyhedra of the zircon and reidite structures is given in Table II using the equilibrium unit cells obtained in our LDA calculations at zero pressure, the corresponding volumes being shown in Table III. The RT experimental values collected in these tables are easily derived from the unit-cell geometries provided by Hazen and Finger[2] and by Kusaba *et al.*[12] for the zircon and reidite structures, respectively. For the tetrahedra considered in this work the four distances d_i are equal, whereas two different angles θ_i and θ'_i with multiplicities 2 and 4, respectively, are found. Both angles are shown in Table II for each polyhedron although it is to be noted that they are related through the equation $\cos\theta_i + 2\cos\theta'_i = -1$.

According to our calculations, the ZrO_4 tetrahedra are rather distorted in both phases, the degree of distortion being smaller in reidite. On the contrary, SiO_4 are rather regular tetrahedra in both phases. The picture emerging from the experimental results is similar, although the distortion of

TABLE II. Zero-pressure structure and distortion parameters of elementary polyhedra of zircon and reidite according to present LDA calculations. Second rows contain values derived from the experimental data of Refs. 2 (zircon) and 12 (reidite). d_i in Å, angles in degree, and $\sigma^2_{\theta,i}$ in degree^2. The multiplicity of θ_i (θ'_i) is 2 (4).

		Zircon				Reidite			
		d_i	θ_i, θ'_i	λ_i	$\sigma^2_{\theta,i}$	d_i	θ_i, θ'_i	λ_i	$\sigma^2_{\theta,i}$
SiO_4	LDA	1.622	96.86, 116.12	1.024	99.03	1.648	120.29, 104.35	1.018	67.87
	Expt.	1.623	96.97, 116.06	1.024	97.31	1.655	127.20, 101.40	1.052	177.8
$ZrO_4(o)$	LDA	2.127	157.58, 92.17	1.618	1165	2.143	134.99, 98.43	1.115	358.0
	Expt.	2.129	157.29, 92.22	1.605	1153	2.129	139.56, 96.86	1.169	489.3
$ZrO_4(p)$	LDA	2.257	65.04, 135.31	1.356	1324	2.243	74.74, 129.17	1.200	792.8
	Expt.	2.267	64.82, 135.46	1.361	1338	2.259	66.25, 134.54	1.333	1250

SiO_4 tetrahedron in reidite is now a little greater than in zircon. We conclude that the more efficient ionic packing in the reidite structure can be associated with the higher regularity of its Zr^{4+} polyhedra, which in turn produces an increasing in the average number of next-nearest neighbors[40] and a decrease in the unit-cell volume. To the best of our knowledge, no other theoretical or experimental analyses of this type has been performed for the cationic polyhedra of the $ZrSiO_4$ polymorphs, with the exception of that by Mursic *et al.* for zircon.[38] The RT experimental values around 2.11 Å^3, 2.47 Å^3, 3.61 Å^3, and 19.1 Å^3 inferred from the figures of their paper for SiO_4, $ZrO_4(o)$, $ZrO_4(p)$, and ZrO_8, respectively, are very similar to those appearing in Table III.

Finally, we complete the zero-pressure description of the ZrO_8 polyhedron with the O(o)-Zr-O(p) angles (θ_l), where O(o) and O(p) are oxygens belonging to the oblate and prolate tetrahedra, respectively. These angles are (experimental values in parentheses and multiplicities m_l in brackets): 68.69° (68.95°) [4], 80.56° (80.43°) [8], and 133.73° (133.77°) [4] for zircon and 71.06° (73.73°) [4], 73.51° (72.61°) [4], 75.16° (77.10°) [4], and 149.84° (143.34°) [4] for reidite. Note that $\Sigma_l m_l \cos\theta_l = 0$ for these O(o)-Zr-O(p) angles and notice also the change in the multiplicity from 8 to 4+4 in passing from zircon to reidite.

TABLE III. Zero-pressure volumes and compressibilities of elementary polyhedra of zircon and reidite according to present LDA calculations [κ_0 is 4.33 for zircon and 3.88 for reidite (in 10^{-3} GPa^{-1} units); see Table I]. Second rows contain values derived from the experimental data of Refs. 2 (zircon) and 12 (reidite). f_i stands for the occupation factor of the corresponding polyhedron (V_i/V). V_i in Å^3 and κ_i in 10^{-3} GPa^{-1} units.

		Zircon			Reidite		
Polyhedron		V_i	f_i	κ_i	V_i	f_i	κ_i
SiO_4	LDA	2.113	0.033	2.89	2.235	0.038	2.25
	Expt.	2.118	0.032	4.4	2.154	0.037	
$ZrO_4(o)$	LDA	2.399		4.48	4.289		2.16
	Expt.	2.434			3.913		
$ZrO_4(p)$	LDA	3.737		2.37	4.403		4.72
	Expt.	3.769			3.844		
ZrO_8	LDA	18.862	0.291	4.55	18.663	0.321	4.20
	Expt.	19.004	0.291	3.6	18.699	0.318	
O_6 voids	LDA	43.90	0.676	4.30	37.16	0.641	3.81
	Expt.	44.08	0.677	4.75	38.03	0.645	

Overall, the qualitative image of the shape and orientation of SiO_4 and ZrO_8 polyhedra in the cell is not modified up to at least 60 GPa in each of the two polymorphs. We believe that a quantitative analysis of the pressure effects on distances and angles of these polyhedra may be also worth to be performed. According to our calculations, the Si-O distances and the degree of distortion of the SiO_4 tetrahedra of zircon and reidite decrease as pressure increases: $d=1.581$ Å, $\theta=97.46°$, $\lambda=1.022$, and $\sigma^2_\theta=89.71$ deg^2 for zircon and $d=1.613$ Å, $\theta=118.74°$, $\lambda=1.014$, and $\sigma^2_\theta=50.04$ deg^2 for reidite, at about 30 GPa. In zircon, the difference between the two sets of Zr-O distances becomes larger as pressure is applied (0.17 Å at p around 30 GPa to be compared with 0.13 Å at $p=0$). This behavior of the Zr-O distances induces a more strained ZrO_8 dodecahedra at increasing pressure, thus reducing the stability of the zircon polymorph, an argument in line with the analysis performed by Mursic *et al.*[38] in their high-temperature study of zircon. On the contrary, the calculations show that the difference between the Zr-O distances in reidite decreases as pressure increases (0.06 Å at $p\simeq 30$ GPa to be compared with 0.10 Å at $p=0$). The θ angles of the ZrO_4 tetrahedra at about 30 GPa differ less than 1% from those at $p=0$ shown in Table II, with the exception of $\theta_{ZrO_4(p)}$ in reidite which is 3% higher. Concerning the O(o)-Zr-O(p) angles (θ_l), we found that the values at 30 GPa differ from those at $p=0$ only around 1%.

C. EOS: Polyhedral interpretation and AIM picture

A microscopic analysis of the compressibility of zircon and reidite (κ) is performed now in terms of the polyhedral and atomic compressibilities (κ_i) and occupation factors (f_i). The compressibility of polyhedron (atom) i is defined as $\kappa_i = -\partial \ln V_i/\partial p$, and the occupation factor of i as the ratio between the volume occupation of that polyhedron (atom) [$n_i \times V_i$, n_i being the number of i polyhedra (atoms) per formula unit] and the volume per formula unit (V). As a consequence, the polyhedral (atomic) volumes and compressibili-

ties, and the crystal volume and compressibility, can be written as follows (see Refs. 41–43):

$$V_i = V\frac{f_i}{n_i}, \quad \kappa_i = \kappa - \frac{\partial \ln f_i}{\partial p}, \quad V = \sum_i n_i V_i, \quad \kappa = \sum_i f_i \kappa_i. \tag{3}$$

The analysis of the polyhedral contributions to the crystal compressibility has to be performed in terms of the compressibilities and occupation factors of SiO_4 and ZrO_8 polyhedra and also noting that O_6 octahedral voids complete the unit-cell volume. This compressibility decomposition is not possible using $ZrO_4(p)$ and $ZrO_4(o)$ tetrahedra because they (and obviously ZrO_8) share common regions of space in the cell. f_{SiO_4} and f_{ZrO_8} are functions of the oxygen coordinates $\vec{x}$, where $\vec{x}$ contains the set of coordinates of O atoms in general positions $[(y^z, z^z)$ for O in zircon and (x^r, y^r, z^r) for O in reidite]. In the case of zircon, the expressions for $f^z_{SiO_4}$ and $f^z_{ZrO_8}$ are

$$f^z_{SiO_4} = \frac{2}{3}\left(\frac{1}{2} - 2y^z\right)\left(4y^z z^z - z^z - \frac{3}{2}y^z + \frac{3}{8}\right),$$

$$f^z_{ZrO_8} = \frac{1}{3}(4y^z + 1)(y^z + 2z^z) + \frac{1}{24}(1 - 4y^z)(1 + 4y^z)(1 + 8z^z). \tag{4}$$

We omit larger expressions for reidite.

Table III shows the zero-pressure properties of elementary polyhedra of zircon and reidite obtained from our LDA calculations as well as the values derived from available experimental information. Table III also includes the properties associated with the O_6 voids. In zircon, the calculated polyhedral compressibilities ($\kappa_{SiO_4,0}=2.89$ and $\kappa_{ZrO_8,0}=4.55$ in 10^{-3} GPa^{-1} units) confirm the criticisms of Smyth *et al.*,[8] with respect to the anomalous values reported by Hazen and Finger ($\kappa_{SiO_4,0}=4.4\pm1.1$, $\kappa_{ZrO_8,0}=3.6\pm0.6$),[2] and support the analysis of the experimental data of Scott *et al.*[5] in reidite, though our $B_{SiO_4,0}$ ($=1/\kappa_{SiO_4,0}$) value around 450 GPa is not as high as the value (>700 GPa) quoted for this polyhedron. In both structures, the volume occupied by the dodecahedra is almost 9 times greater than that of the tetrahedra and, thus, the total contribution ($f_i\kappa_i$) of ZrO_8 to the crystal compressibility is much more important than that of SiO_4. We must note, however, that the contribution of the voids to the volume reduction of zircon and reidite under hydrostatic pressure is about twice that of the ZrO_8 polyhedra, because both phases are relatively open structures. Then, although the average compressibility of the voids is slightly smaller than that of ZrO_8 in both structures, the total contribution of the voids to the bulk compressibility becomes dominant. It is also remarkable that, according to the polyhedral picture, about 98% of the volume difference between zircon and reidite structures can be explained as due to the lower volume occupied by the O_6 voids in reidite (see Table III). The small size and low compressibility of the SiO_4 tetrahedra make them to play an almost negligible role in the crystal response to pressure. Finally, note that the compressibilities shown in Table III for the ZrO_4 tetrahedra are in concordance with the discussion at the end of Sec. III B.

TABLE IV. Calculated atomic volumes (V_i in $Å^3$) and compressibilities (κ_i in 10^{-3} GPa^{-1}) (i=Si, Zr, and O) in zircon and reidite according to the present zero-pressure LDA calculations. f_i stands for the occupation factor of the corresponding atom.

	Zircon			Reidite		
Atom	V_i	f_i	κ_i	V_i	f_i	κ_i
Si	3.53	0.054	4.90	3.11	0.054	4.64
Zr	9.00	0.138	3.36	9.02	0.155	2.89
O	13.1	0.808	4.65	11.5	0.791	4.12

The LDA-calculated pressure effects on the oxygen coordinates depicted in Fig. 3(b) lead to $f_{SiO_4}(p)$ and $f_{ZrO_8}(p)$ functions with slopes of different sign and magnitude in both polymorphs, negative and small for the ZrO_8 curves (average decreasing of about 1% from 0 to 60 GPa) and positive and much greater for the SiO_4 curves (average increasing of about 5% in the same range of pressure). This behavior and Eqs. (3) show that (i) $\kappa_{SiO_4} < \kappa < \kappa_{ZrO_8}$ for all pressures studied (up to 60 GPa), (ii) the compressibilities of the bulk and the dodecahedra are similar in both structures, in concordance with the findings of Errandonea *et al.*[36] quoted above, and (iii) the average of the compressibilities of these two types of polyhedra is not a good estimation of the compressibility of $ZrSiO_4$, contrarily to AB_2O_4 spinels.[44]

The AIM analysis of the electron density of zircon and reidite provides further insight into the compressibility of these systems. The relevant properties at zero pressure appear summarized in Table IV. First, according to the calculated κ_i values, Zr is more difficult to compress than O and this atom is slightly less compressible than Si in both structures, κ_O being about 6–7% higher than the compressibility of the bulk. Besides, the three atoms are expected to be a little more difficult to compress in reidite than in zircon. κ_O in these systems (4.65×10^{-3} GPa^{-1} in zircon and 4.12×10^{-3} GPa^{-1} in reidite) is smaller than in the AB_2O_4 (A=Mg,Zn; B=Al,Ga) spinels where $\kappa_O \sim 5.0\times10^{-3}$ GPa^{-1} and, in contrast to zircon and reidite, O is the most compressible ion in the crystal.[45] On the contrary, the relative compressibility of O and Si in zircon and reidite is analogous to that previously inferred for N and Si in β- and γ-Si_3N_4.[35] Second, according to our calculations, V_O is 1.3–1.5 times V_{Zr} and 3.7 times V_{Si}, the oxygen atoms dominating the unit-cell space mainly due to the stoichiometry of the unit cell (see f_i values in Table IV). As a consequence, the bulk compressibility of zircon and reidite ($\kappa=\Sigma_i f_i\kappa_i$) becomes mainly determined by the compressibility of oxygen, as in AB_2O_4 spinels[45] and in the same way as the bulk compressibility of β- and γ-A_3N_4 (A=C,Si,Ge) becomes determined by the compressibility of N.[35] Moreover, as $V=\Sigma_i n_i V_i$, we can see from Table IV that 95% of the volume difference between zircon and reidite is due, in the AIM picture, to the lower volume occupied by O in the reidite structure. This result is in agreement with that shown above in terms of the consti-

tutive polyhedra, where the O_6 voids were found to be the main responsible of the volume difference between both phases.

D. Relative stability and phase transitions properties

$ZrSiO_4$ is known to display a pressure-induced first-order phase transition from zircon to reidite. At elevated temperatures, $ZrSiO_4$ decomposes into its simple oxides, very likely β-crystoballite SiO_2 and tetragonal ZrO_2 at zero pressure[38] or stishovite SiO_2 and cottunite-type ZrO_2 at high pressure.[14] There is a good deal of experimental data[1,3,4,6,9–14,38,46] concerning both thermodynamic and mechanistic aspects of these transformations and less information from the theoretical side.[30,31] The experimental information collected so far clearly shows that the zircon→reidite and $ZrSiO_4 \rightarrow ZrO_2 + SiO_2$ transformations are kinetically hindered. Thus, we should bear in mind this fact to analyze the difference between our calculated thermodynamic (equilibrium) transition pressures (p_t) and the experimental ones ($p_{t,expt}$). When the parent and product phases are close to equilibrium, the energetic barriers associated with these transformations can be overcome only at sufficiently high temperatures, and then observed transition pressures may be compared with the thermodynamic ones. From the high temperature data[4,9,10] and assuming a positive Clapeyron slope for the former transformation,[1,6] the experimental transition pressure is expected to be below 10 GPa at room temperature. Our LDA static value of around 5.3 GPa is in concordance with this expectation and is also in good agreement with the calculated values of Crocombette and Ghaleb[30] and Farnan *et al.*[31] In addition, a decrease in the volume of $ZrSiO_4$ of 10.3% for this transformation at p_t has been obtained (see arrow at 5.3 GPa in Fig. 2), a value very close to the calculated (LDA) and experimental ones at zero pressure [10.5% and about 10–11%, respectively (see Table I)]. Besides, a relative volume change of around 8.9% has been also obtained for the $ZrSiO_4$(reidite)→ZrO_2(cottunite-type)+SiO_2(stishovite) decomposition at its computed equilibrium pressure (6.3 GPa). Both transformations exhibit an increase of the bulk modulus at the corresponding transition pressures that can be explained as mainly due to the volume reduction.

We have also explored the effect of temperature in the equilibrium pressure boundaries of these two transformations. The addition of vibrational energy and entropy contributions to the static results was performed with the Debye model. We have found a qualitatively satisfactory picture with both Clapeyron slopes slightly positive in the temperature ranges covered by our calculations: p_t increases 1.9 GPa from 0 to 1800 K for zircon→reidite transformation, whereas in the $ZrSiO_4$(reidite)→ZrO_2(cottunite-type)+SiO_2(stishovite) decomposition the increment in p_t is 1.5 GPa in the range 0–1400 K. This means that there is a small decrease of entropy associated with these transitions, supporting the exhaustive analysis of Finch and Hanchar in many ABO_4 compounds including $ZrSiO_4$.[6]

Finally, the study of post-scheelite phases of $ZrSiO_4$ has been performed by computing the fergusonite- and wolframite-type structures of this compound. They belong, respectively, to the $I2/a$ and $P2/c$ monoclinic space groups. We used two different sets of starting cell parameters and atomic positions in the geometrical optimization of the fergusonite-type structure. The first one corresponds to a slightly distorted scheelite-type phase, derived from the $I4_1/a$-$I2/a$ group-subgroup relationships, and the second one to structures having a $P2_1/c$ space group. This latter strategy allows us to explore a possible relaxation of the $I2/a$ structure of $ZrSiO_4$ to the $P2_1/c$ symmetry, a feature noted by Sen *et al.* in $LiYF_4$ from their molecular dynamics simulations.[47] According to our first strategy, the optimal structures always correspond to the scheelite-type lattice, but according to the second one, they correspond to the scheelite-type lattice in the volume regime from about 51 to 56 Å^3 and to the wolframite-type phase in the volume regime from about 47 to 50 Å^3. Then, full geometrical optimizations of this latter structure have been carried out at several volumes in the range 47 Å$^3 \leq V \leq 65$ Å^3. The energy-volume curve obtained shows a minimum at V_0=56.71 Å^3 and around 50 kJ/mol higher in energy than that of the reidite structure at zero pressure. Furthermore, an hypothetical reidite→wolframite-type structure phase transition is predicted at a pressure about 62 GPa, well beyond the decomposition of $ZrSiO_4$ into its simple oxides.

IV. CONCLUSIONS

We presented a combined theoretical and experimental analysis of the structure and stability of $ZrSiO_4$ under hydrostatic pressure, with emphasis on the zircon⇌reidite phase transition. Our LDA calculations provide an accurate overall description of the behavior of this system. Both LDA calculations and our diamond-anvil cell experiments give a B_0 value for zircon around 230 GPa, thus supporting the experimental and theoretical results included in set I discussed above. Since recent static compression data yield B_0 values around 10% lower, we suggest that ultrasonic measurements on synthetic pure zircon were performed in order to determine elastic constants and bulk modulus. Our LDA value of B_0 for reidite (258 GPa) is much smaller than that obtained by Ono *et al.* (around 400 GPa),[4] about 14% smaller than the value reported by Scott *et al.*,[5] but within the range of values predicted recently by Errandonea *et al.* from the compressibility of ZrO_8 polyhedra (220±40 GPa).[36] LDA calculations inform that ZrO_8 polyhedra compress at a similar rate as that of the bulk in both zircon and reidite. According to the AIM picture, Zr is more difficult to compress than O and this atom is slightly less compressible than Si in both zircon and reidite. Interestingly, the bulk compressibility of these structures becomes determined by the O_6 voids and the oxygen atoms, according to the polyhedral and AIM analyses, respectively. In agreement with the available experimental information, the degree of structural anisotropy under pressure obtained for zircon is greater than that of reidite, the linear compressibility of the former along the a (c) axis being greater (smaller) than that along c (a). The calculated static equilibrium transition pressure for this transformation (5.3 GPa) agrees reasonably with the equilibrium experimental value inferred at room conditions from the high-

temperature experimental data. Finally, a decomposition of $ZrSiO_4$ into ZrO_2 (cottunite) and SiO_2 (stishovite) is predicted at about 6 GPa.

ACKNOWLEDGMENTS

Financial support from the Spanish DGICYT, Project No. BQU2003-06553, is gratefully acknowledged by M.M., M.F., and J.M.R. Part of this work was performed during the stay of J.M.R. at the Laboratoire de Chimie Physique (Université Pierre et Marie Curie, Paris) under a HPC-EUROPA grant for computational use of IDRIS resources. We thank HASYLAB-DESY for permission to use the synchrotron radiation facility. L.G. and J.S.O. acknowledge financial support from the Danish Natural Sciences Research Council through DANSYNC. We thank D. Errandonea for sending us a copy of Ref. 36 before publication.

*Corresponding author. Electronic address: mateo@fluor.quimica.uniovi.es

[1] E. Knittle and Q. Williams, Am. Mineral. **78**, 245 (1993).
[2] R. M. Hazen and L. W. Finger, Am. Mineral. **64**, 196 (1979).
[3] W. van Westrenen, M. R. Frank, J. M. Hanchar, Y. Fei, R. J. Finch, and C.-S. Zha, Am. Mineral. **89**, 197 (2004).
[4] S. Ono, Y. Tange, I. Katayama, and T. Kikegawa, Am. Mineral. **89**, 185 (2004).
[5] H. P. Scott, Q. Williams, and E. Knittle, Phys. Rev. Lett. **88**, 015506 (2002).
[6] R. J. Finch and J. M. Hanchar, in *Zircon*, edited by J. M. Hanchar and P. W. O. Hoskin [Rev. Mineral. Geochem. **53**, 1 (2003)].
[7] W. C. Tennant, R. F. C. Claridge, C. J. Walsby, and N. S. Lees, Phys. Chem. Miner. **31**, 203 (2004).
[8] J. R. Smyth, S. D. Jacobsen, and R. M. Hazen, in *High-Temperature and High-Pressure Crystal Chemistry*, edited by R. M. Hazen and R. T. Downs [Rev. Mineral. Geochem. **41**, 187 (2000)].
[9] A. F. Reid and A. E. Ringwood, Earth Planet. Sci. Lett. **6**, 205 (1969).
[10] L. Liu, Earth Planet. Sci. Lett. **44**, 390 (1979).
[11] K. Kusaba, Y. Syono, M. Kikuchi, and K. Fukuoka, Earth Planet. Sci. Lett. **72**, 433 (1985).
[12] K. Kusaba, T. Yagi, M. Kikuchi, and Y. Syono, J. Phys. Chem. Solids **47**, 675 (1986).
[13] H. Leroux, W. U. Reimold, C. Koeberl, U. Hornemann, and J.-C. Doukhan, Earth Planet. Sci. Lett. **169**, 291 (1999).
[14] Y. Tange and E. Takahashi, Phys. Earth Planet. Inter. **143**, 223 (2004).
[15] R. F. W. Bader, *Atoms in Molecules* (Oxford University Press, Oxford, 1990).
[16] J. S. Olsen, Rev. Sci. Instrum. **83**, 1058 (1992).
[17] H. K. Mao, J. Xu, and P. M. Bell, J. Geophys. Res. **91**, 4673 (1986).
[18] F. J. Birch, J. Appl. Phys. **9**, 279 (1938); Phys. Rev. **71**, 809 (1947).
[19] G. Kresse and J. Furthmuller, Phys. Rev. B **54**, 11169 (1996).
[20] G. Kresse and D. Joubert, Phys. Rev. B **59**, 1758 (1999).
[21] J. P. Perdew and Y. Wang, Phys. Rev. B **45**, 13244 (1992).
[22] D. M. Ceperley and B. J. Alder, Phys. Rev. Lett. **45**, 566 (1980).
[23] H. J. Monkhorst and J. D. Pack, Phys. Rev. B **13**, 5188 (1976).
[24] M. A. Blanco, E. Francisco, and V. Luaña, Comput. Phys. Commun. **158**, 57 (2004).
[25] J. L. Fleche, Phys. Rev. B **65**, 245116 (2002).
[26] A. Martín Pendás and V. Luaña, computer code CRITIC, 1995–2003.
[27] V. R. Saunders, R. Dovesi, C. Roetti, M. Causá, N. M. Harrison, R. Orlando, and C. M. Zicovich-Wilson, *CRYSTAL98 User's Manual* (University of Torino, Torino, 1998).
[28] H. Ozkan, Phys. Chem. Miner. **2**, 215 (1978).
[29] S. Rios and T. Boffa-Ballaran, J. Appl. Crystallogr. **36**, 1006 (2003).
[30] J. P. Crocombette and D. Ghaleb, J. Nucl. Mater. **257**, 282 (1998).
[31] I. Farnan, E. Balan, C. J. Pickard, and F. Mauri, Am. Mineral. **88**, 1663 (2003).
[32] M. J. Akhtar and S. Waseem, Solid State Sci. **5**, 541 (2003).
[33] R. Devanathan, L. R. Corrales, W. J. Weber, A. Chartier, and C. Meis, Phys. Rev. B **69**, 064115 (2004).
[34] H. Ozkan, L. Cartz, and J. C. Jamieson, J. Appl. Phys. **45**, 556 (1974).
[35] M. Marqués, J. Osorio, R. Ahuja, M. Flórez, and J. M. Recio, Phys. Rev. B **70**, 104114 (2004).
[36] D. Errandonea, J. Pellicer-Porres, F. J. Manjón, A. Segura, Ch. Ferrer-Roca, R. S. Kumar, O. Tschauner, P. Rodríguez-Hernández, J. López-Solano, S. Radescu, A. Mújica, A. Muñoz, and G. Aquilanti, Phys. Rev. B **72**, 174106 (2005).
[37] W. van Westrenen, M. R. Frank, Y. Fei, J. M. Hanchar, R. J. Finch, and C.-S. Zha, J. Am. Ceram. Soc. **88**, 1345 (2005).
[38] Z. Mursic, T. Vogt, and F. Frey, Acta Crystallogr., Sect. B: Struct. Sci. **48**, 584 (1992).
[39] K. Robinson, G. V. Gibbs, and P. H. Ribe, Science **172**, 567 (1971).
[40] X. Wang, I. Loa, K. Syassen, M. Hanfland, and B. Ferrand, Phys. Rev. B **70**, 064109 (2004).
[41] M. Calatayud, P. Mori-Sánchez, A. Beltrán, A. Martín Pendás, E. Francisco, J. Andrés, and J. M. Recio, Phys. Rev. B **64**, 184113 (2001).
[42] L. Gracia, A. Beltrán, J. Andrés, R. Franco, and J. M. Recio, Phys. Rev. B **66**, 224114 (2002).
[43] P. Mori-Sánchez, M. Marqués, A. Beltrán, J. Z. Jiang, L. Gerward, and J. M. Recio, Phys. Rev. B **68**, 064115 (2003).
[44] J. M. Recio, R. Franco, A. Martín Pendás, M. A. Blanco, L. Pueyo, and R. Pandey, Phys. Rev. B **63**, 184101 (2001).
[45] A. Martín Pendás, Aurora Costales, M. A. Blanco, J. M. Recio, and Víctor Luaña, Phys. Rev. B **62**, 13970 (2000).
[46] B. P. Glass, S. Liu, and P. B. Leavens, Am. Mineral. **87**, 562 (2002).
[47] A. Sen, S. L. Chaplot, and R. Mittal, Phys. Rev. B **68**, 134105 (2003).